24th ABCM International Congress of Mechanical Engineering
December 3-8, 2017, Curitiba, PR, Brazil

COBEM-2017- 0971
EXPERIMENTAL STUDY OF A HYDRAULIC ENGINE MOUNT WITH EMPHASIS ON DECOUPLER CHARACTERISTICS

Angelo Marcelo Tusset
Bianca Marin
Frederic Conrad Janzen
Federal University of Technology – Paraná, 84016-210, Ponta Grossa – PR, Brazil
tusset@utfpr.edu.br; bi_marin@hotmail.com; fcjanzen@hotmail.com

José Manoel Balthazar
ITA - Aeronautics Technological Institute, Marechal Eduardo Gomes Square, 12228-900, São José dos Campos – SP, Brazil
jmbaltha@gmail.com

Eduardo M. O Lopes
Carlos Alberto Bavastri
Federal University of Paraná, 81531-980, Curitiba- PR, Brazil
eduardo lopes@ufpr.br; bavastri@ufpr.br

Abstract. *This paper investigates the influence of the decoupler geometry in the dynamic characteristics of the system. The parameters evaluated are the dynamic stiffness and phase angle of the system if the central geometry of the decoupler changes, keeping the gap with the plates. The investigation is based on tests results and the mathematical model of both situations will be investigated. All hydraulic mounts reported in the literature are conceptually similar but differ in detailed structural design as conduced in this paper.*

Keywords: *Hydraulic Engine Mount, vibration isolation, peak frequency, dynamic stiffness, decoupler function.*

1. INTRODUCTION

The vehicle engine mounting system, generally, consists of an engine (vibration source) and several mounts connected to the vehicle structure (Yu *et al*., 2001). The engine mount system has the function to support the weight of the engine as well as to isolate drive and passenger from the vibration and noise generated by the engine. Undesirable vibrations come from two different sources: road-induced vibrations, providing high-amplitude and low-frequency, and engine-induced vibrations, of low-amplitude and high-frequency (Geisberger *et al*., 2002).

Hydraulic engine mounts are effective passive vibration isolation devices used to isolate these two distinct modes of vibration. The ideal mount is desired to have high stiffness and damping characteristics for low-frequency and high-amplitude vibrations (usually greater than 0.3 mm in amplitude at 1 to 50 Hz), whereas for high-frequency and small-amplitude vibrations the stiffness and damping characteristics are low (amplitudes less than 0.3 mm at 50-300 Hz), see (Geisberger *et al*., 2002; Golnaraghi and Jazar, 2001).

These targets are met by a hydraulic mount due to use of a device referred to as decoupler in conjunction with a passage knows as the inertia track (Christopherson and Jazar, 2006).

This common passive isolator is the focus of this paper and is illustrated in Fig. 1.

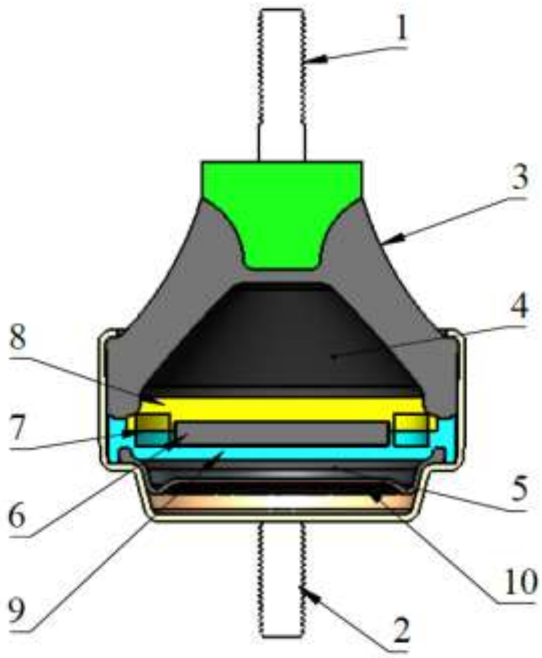

Figure 1. Cross section of the hydraulic engine mount

The connection of the hydraulic mount with the engine and chassis is made through studs (1) and (2). The main rubber (3) supports the static engine weight. The top chamber (4) and lower chamber (5) are filled with fluid, usually an ethylene glycol mixture of antifreeze and water.

The fluid flows through the two chambers according to the engine motion. The volumetric displacement of the fluid is partially absorbed by the decoupler (6) and the remaining portion is forced to flow through the inertia track (7).

The decoupler is allocated between the upper plate (8) and lower plate (9), and may move freely. For small amplitude excitations, the fluid passes primarily through the decoupler with low resistance, and for large excitations the fluid is forced through the higher resistance inertia track.

The diaphragm (10) is a thin rubber that allows the lower chamber to expand or contract.

2. EXPERIMENTAL PROCEDURE

In order to evaluate the dynamic characteristics of the system, two geometric configurations of the decoupler were tested: without and with a small hole.

(a) (b)

Figure 2. (a) Decoupler without hole. (b) Decoupler with a small hole.

The experiment was carried out in a MTS machine, using a hydraulic cylinder driven via the servo-controlled actuator. The linear motion of the actuator displaces fluid into a two-chamber. High-frequency-pressure sensors are used to collect output data.

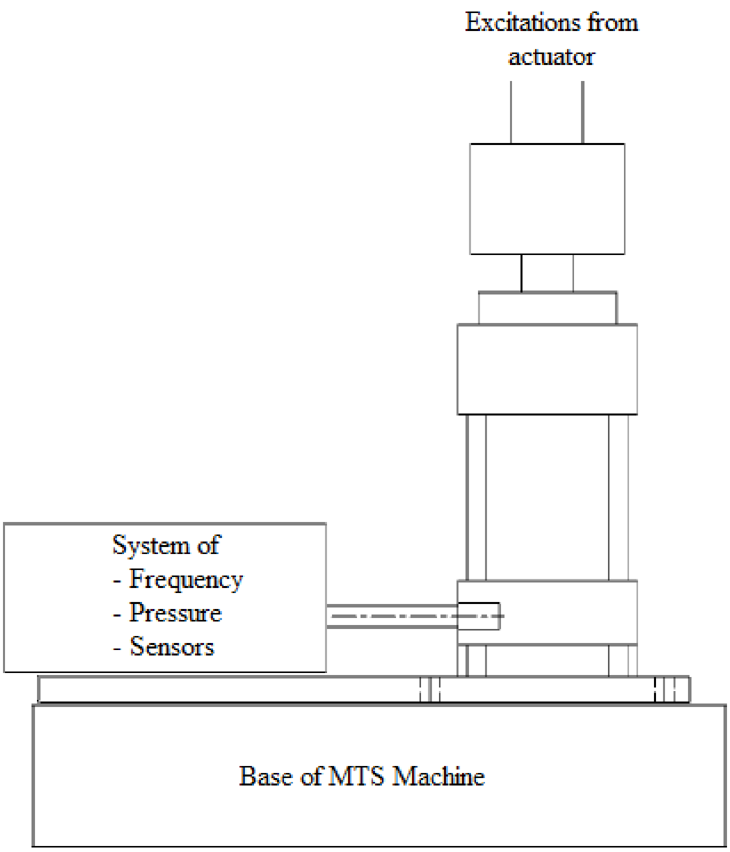

Figure 3. Schematic of experimental apparatus.

2.1 Experimental results

Figure 4 shows the dynamic behavior of the system – stiffness curves and phase angle curves - with different decoupler designs.

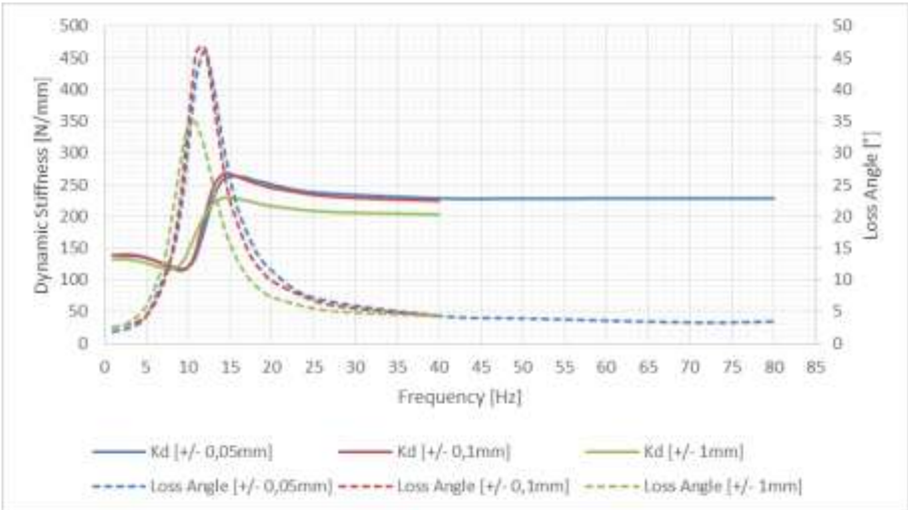

(a)

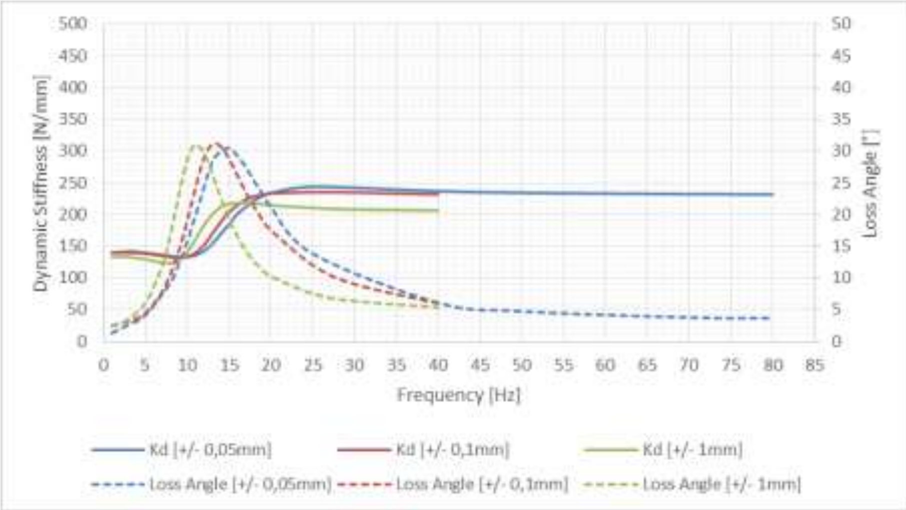

(b)

Figure 4. (a) Dynamic characterization – decoupler without hole. (b) Dynamic characterization – decoupler with a small hole.

Figure 5 shows static characterization for the different decoupler designs.

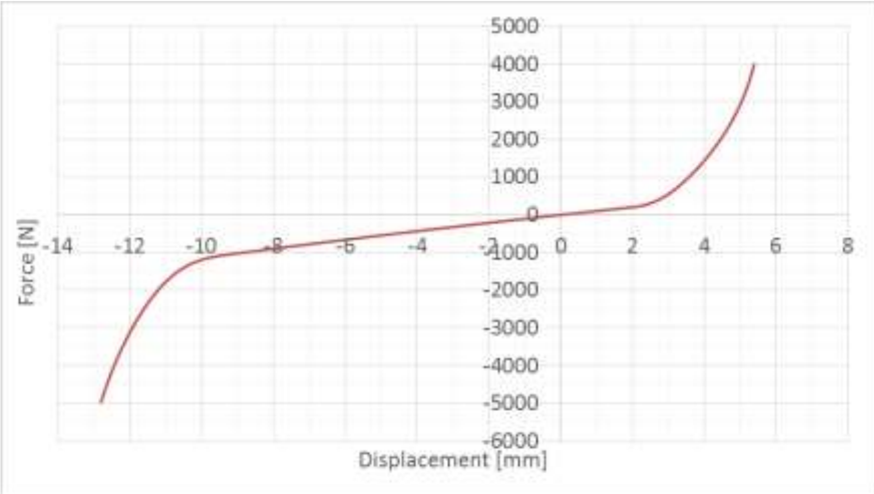

(a)

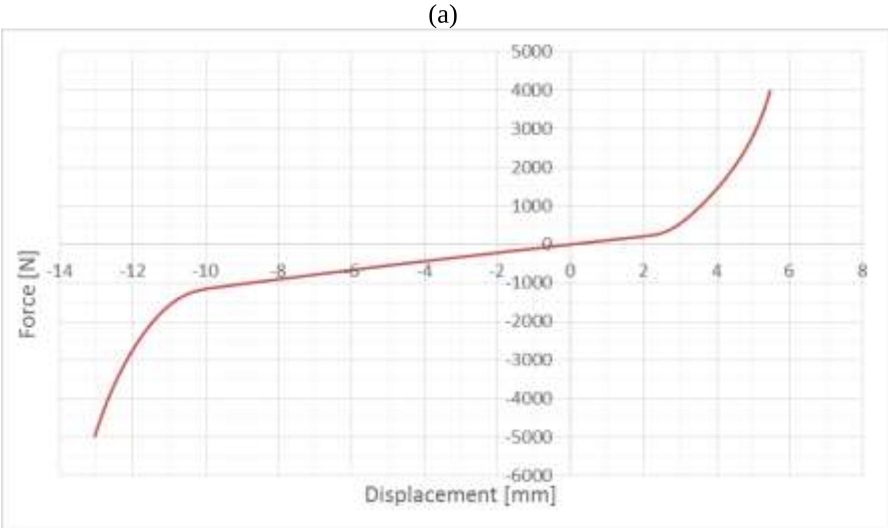

(b)

Figure 5. (a) Static characterization – decoupler without hole. (b) Dynamic characterization – decoupler with a small hole.

In Figs. 4 and 5 it is observed the influence that the small hole in the decoupler causes in the dynamic characteristics of the system. When the hole is present, the phase angle decreases for small amplitudes whereas the stiffness curve is softer. The peak of phase angle corresponds to the resonance frequency of the slug of the fluid that is flowing back and forth in the inertia track, against the bulge stiffness of the elastomeric chambers. The dynamic stiffness is reduced after resonance due to the reduction in upper-chamber pressure.

2.2 Coefficient of rigidity (K) and damping coefficient (C)

In Figs. 6 and 7, the variation of the rigidity coefficient (K) and the damping coefficient (C) can be observed for the variation of the excitation from 1 Hz to 40 Hz with amplitude of 0.0001 [m].

Figure 7 shows the variation for case of the decoupler without hole.

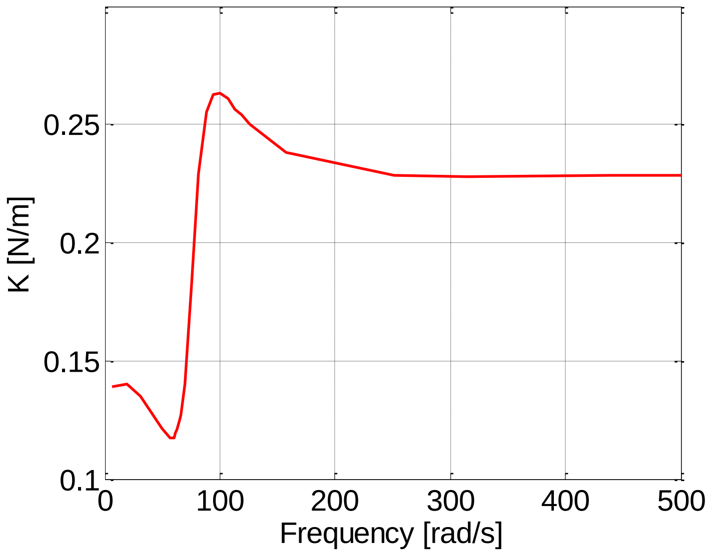

(a)

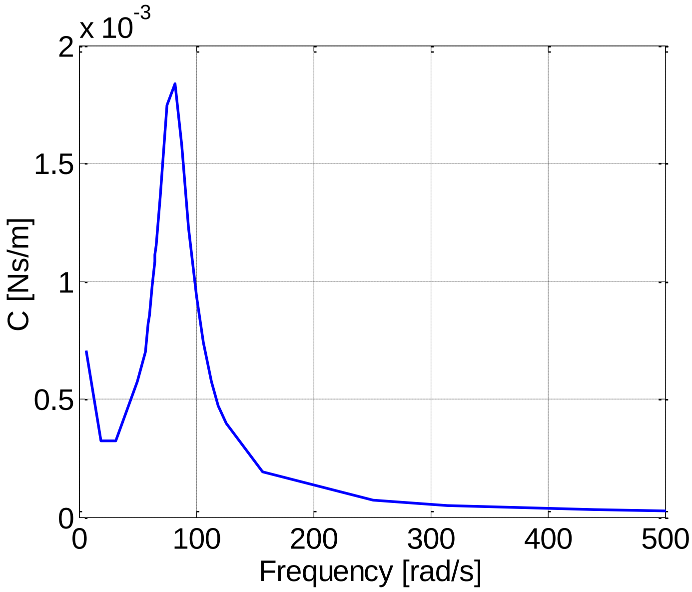

(b)

Figure 6. Decoupler without hole. (a). Coefficient of rigidity ‘K’ vs Frequency of excitation. (b) Damping coefficient C vs Frequency of excitation

As can be seen in Fig. 6, the coefficients k and C depend on the frequency of the excitation. Considering the frequency variation in radians $\omega = [6.2831, 502.6548]$, and the application of curve fitting by the least squares method (Burden and Faires, 2007), we can consider the coefficients $K(\omega)$ and $C(\omega)$ in the following way:

$$K(\omega)=\begin{cases}-10^{-9}\omega^5+3\cdot10^{-7}\omega^4-3\cdot10^{-5}\omega^3+9\cdot10^{-4}\omega^2-1.2\cdot10^{-2}\omega+0.1872 & for\,1\le\omega\le 94.24\\ 6\cdot10^{-12}\omega^4-10^{-8}\omega^3+6\cdot10^{-6}\omega^2-1.4\cdot10^{-3}\omega+0.3546 & for\quad \omega>94.24\end{cases} \tag{1}$$

$$C(\omega)=\begin{cases}-3\cdot10^{-9}\omega^3+10^{-6}\omega^2-5\cdot10^{-5}\omega+0.001 & for\,1\le\omega\le 81.68\\ -6\cdot10^{-15}\omega^5+10^{-11}\omega^4-6\cdot10^{-9}\omega^3+2\cdot10^{-6}\omega^2-2\cdot10^{-4}\omega+0.0127 & for\quad \omega>81.68\end{cases} \tag{2}$$

Figure 7 shows the variation for case of the decoupler with a small hole.

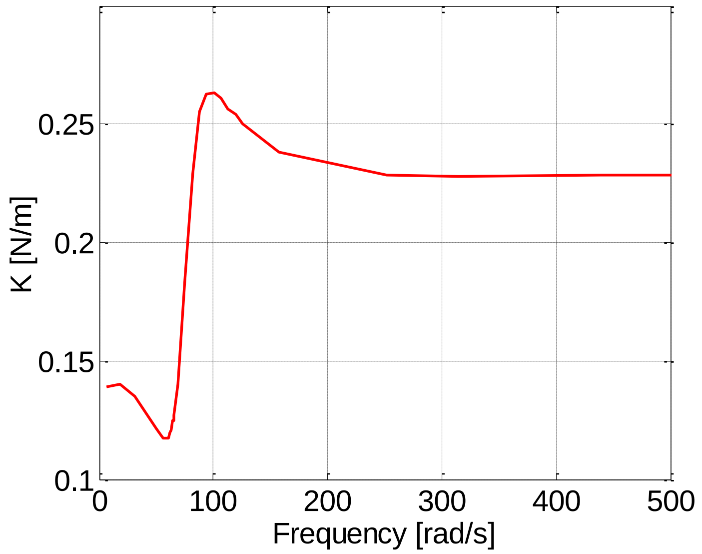

(a)

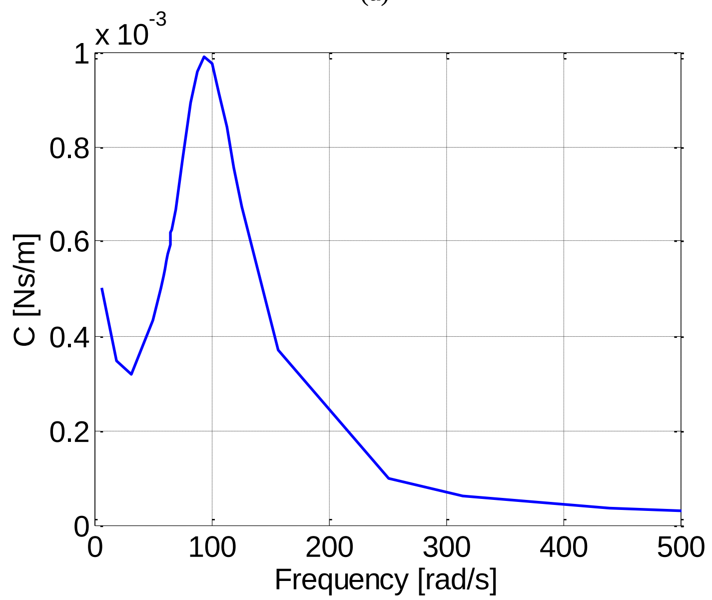

(b)

Figure 7. Decoupler with a small hole. (a). Coefficient of rigidity 'K' vs Frequency of excitation. (b) Damping coefficient C vs Frequency of excitation

Considering the application of curve fitting by the least squares method, we can consider the coefficients $K(\omega)$ and $C(\omega)$ in the following way:

$$K(\omega)=\begin{cases}3\cdot10^{-11}\omega^5-2\cdot10^{-8}\omega^4+3\cdot10^{-6}\omega^3-2\cdot10^{-4}\omega^2+3.8\cdot10^{-3}\omega+0.1196 & for 1\le\omega\le157.08\\ -3\cdot10^{-10}\omega^3+5\cdot10^{-7}\omega^2-2\cdot10^{-4}\omega+0.2681 & for\quad \omega>157.08\end{cases} \tag{3}$$

$$C(\omega)=\begin{cases}-2\cdot10^{-9}\omega^3+5\cdot10^{-7}\omega^2-3\cdot10^{-5}\omega+0.0006 & for 1\le\omega\le94.247\\ 10^{-13}\omega^4-2\cdot10^{-10}\omega^3+10^{-7}\omega^2-3\cdot10^{-5}\omega+0.0032 & for\quad \omega>94.247\end{cases} \tag{4}$$

Eq. (1) to (4) obtained from the least squares method provides a 99.9% correlation with the experimental data. Considering dependence of the stiffness coefficient $K(\omega)$ and the damping coefficient $C(\omega)$, and using the equivalent generalized parameters and applying Newton's second law, the equation of motion of the passive hydraulic isolator is given by:

$$m\ddot{x}+C(\omega)\dot{x}+K(\omega)x=f\cos(\omega t) \tag{5}$$

where: *m* is the total mass of the passive hydraulic isolator, *f* is excitation amplitude, *x* displacement.

3. CONCLUSIONS

As can be seen in Figure 4, the hole in the decoupler membrane makes the loss angle curves decrease for small amplitudes and does not show significant impact for bigger amplitudes of excitation The stiffness influence was smaller than in phase angle curves.

We can also observe that the excitation frequency (ω) changes the coefficients (the stiffness coefficient $K(\omega)$ and the damping coefficient $C(\omega)$). By adjusting the curves it was possible to obtain the coefficient adjustment models (Eq. (1) to (4)) with correlation of 99.9%.

The results obtained from the experimental data provided important information for the application of vibration absorbers in vehicle vibration control.

4. REFERENCES

Burden, R.L., Faires, J. D., 2007, *Numerical analysis*. Cengage Learning.

Christopherson, J. and Jazar G., 2006. "Dynamic behavior comparison of passive hydraulic engine mounts. Part 1: Mathematical analysis". Journal of sound and vibration, Vol. 290, p. 1040-1070.

Geisberger, A., Khajepour, A., and Golnaraghi, F., 2002. "Non-linear modelling of hydraulic mounts: theory and experiment". Journal of sound and vibration, Vol. 249, p. 371-397.

Golnaraghi, M.F. and Jazar, G.N., 2001. "Development and analysis of a simplified nonlinear model of a hydraulic engine mount". Journal of vibration and control, Vol. 7, p. 495-526.

Yu, Y., Naganathan, N.G. and Dukkipati, R.V., 2001. "A literature review of automotive vehicle engine mounting systems". Mechanism and machine theory, Vol. 36, p. 123-142.

5. RESPONSIBILITY NOTICE

The authors are the only responsible for the printed material included in this paper.